Princeton Plasma Physics Laboratory

PPPL-5275

High Resolution Main-ion Charge Exchange Spectroscopy in the DIII-D H-mode Pedestal

B.A. Grierson, K.H. Burrell, C. Chrystal, R.J. Groebner, S.R. Haskey, D.H. Kaplan

July 2016

PRINCETON PLASMA PHYSICS LABORATORY

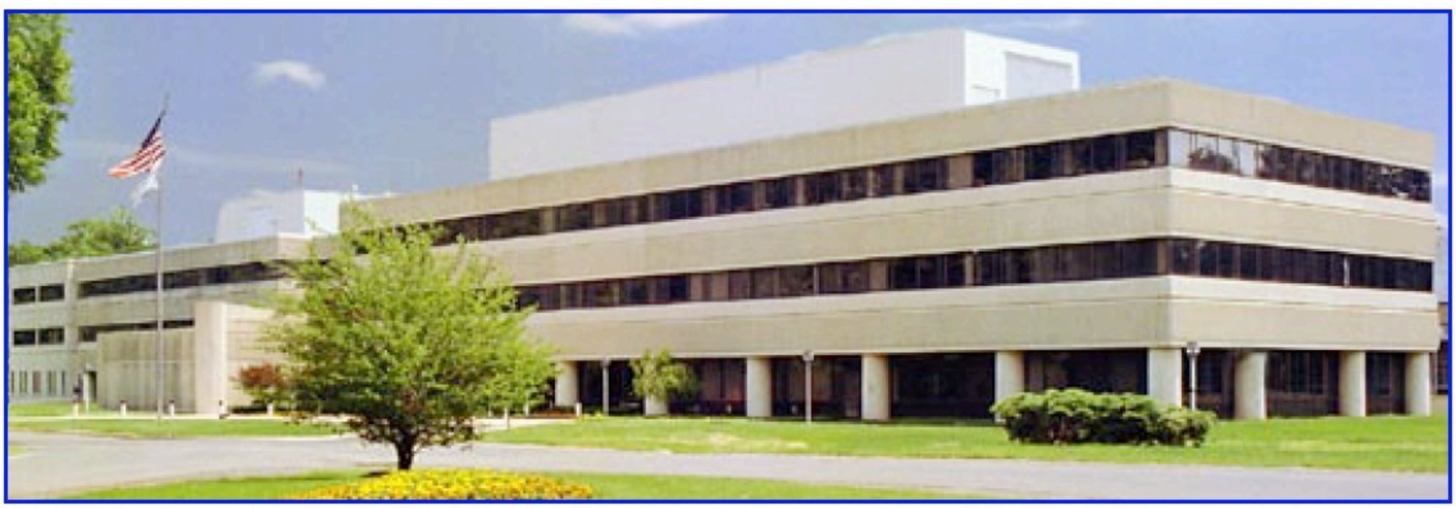

Prepared for the U.S.Department of Energy under Contract DE-AC02-09CH11466.

Princeton Plasma Physics Laboratory
Report Disclaimers

High Resolution Main-ion Charge Exchange Spectroscopy in the DIII-D H-mode Pedestal[a]

B.A. Grierson,[1, b] K.H. Burrell,[2] C. Chrystal,[3] R.J. Groebner,[2] S.R. Haskey,[1] and D.H. Kaplan[2]

[1] *Princeton Plasma Physics Laboratory, Princeton University, Princeton, NJ 08543, USA*

[2] *General Atomics, P.O. Box 85608, San Diego, CA 92186-5608, USA*

[3] *Oak Ridge Associated Universities, Oak Ridge, TN, USA*

(Dated: 18 July 2016)

A new high spatial resolution main-ion (deuterium) charge-exchange spectroscopy system covering the tokamak boundary region has been installed on the DIII-D tokamak. Sixteen new edge main-ion CER sightlines have been combined with nineteen impurity sightlines in a tangentially viewing geometry on the DIII-D midplane with an interleaving design that achieves 8 mm inter-channel radial resolution for detailed profiles of main-ion temperature, velocity, charge-exchange emission and neutral beam emission. At the plasma boundary, we find a strong enhancement of the main-ion toroidal velocity that exceeds the impurity velocity by a factor of two. The unique combination of experimentally measured main-ion and impurity profiles provide a powerful quasi-neutrality constraint for reconstruction of tokamak H-mode pedestals.

I. INTRODUCTION

The beneficial effects of plasma rotation to tokamak stability and transport are well recognized in the magnetic fusion community. As tokamak reactors increase in size, the effectiveness of external actuators such as neutral beam injection to drive rotation decreases dramatically, and the plasma rotation may become dominated by intrinsic torques. In order to understand and eventually predict the plasma rotation profile, the momentum-carrying (main-ion) species' rotation must be measured and compared to first-principles based models. This is especially true in the boundary and pedestal region of the H-mode where the pressure gradient is strong enough to require large differential toroidal rotation between the impurities and main-ions[1]. Furthermore, at the separatrix, kinetic orbits of the main-ions are large enough that phase-space losses produce an edge co-current directed net velocity[2], which is one leading candidate for the generation of net co-current intrinsic rotation[3,4]. This paper describes the design, installation and first profile measurements from a newly commissioned main-ion charge-exchange recombination (CER) spectroscopy system on DIII-D[5] dedicated to the study of deuterium ions in the region between the top of the H-mode pedestal and the plasma scrape-off layer (SOL) beyond the last closed flux surface. This new system increases the coverage of main-ion profiles[6] in DIII-D and expands the operating space of edge main-ion measurements previously covered by plunging mach probes[7] into high-powered H-mode discharges.

[a] Contributed paper published as part of the Proceedings of the 21st Topical Conference on High-Temperature Plasma Diagnostics, Madison, Wisconsin, June, 2016.

[b] Electronic mail: bgriers@pppl.gov

II. DIAGNOSTIC DESIGN

Sixteen new sightlines dedicated to main-ion CER have been installed on the DIII-D tokamak with midplane tangential views of the heating neutral beam line that injects at 330° in machine coordinates. These new sightlines were installed during an upgrade of the previously existing high-resolution edge CER system[8] that expands the radial range of the closely spaced sightlines[9]. Design of the main-ion CER sightlines is tightly coupled to the sightlines dedicated to the impurity measurements because direct comparisons of main-ion and impurity profiles is the primary goal of the diagnostic system. Combining the optics in one viewing port and fiber clamp removes possible overall systematic errors that will occur if the measurements use different clamping or lens systems. To this end, a close-packed array of fused-silica fibers displayed in Fig. 1 has been employed to acquire the tokamak photoemission. Each fiber core has a 750 μm core diameter, and two cores stacked vertically are used for a single sightline to increase the signal without sacrificing radial resolution. The vertical fiber pairs are enclosed in a vertically elongated octagonal block. There are two rows of octagonal blocks where the main-ion system is composed of sixteen blocks, and the impurity system is composed of nineteen blocks. Inside the vacuum vessel, the measurement locations where the sightlines cross the 330° beam are displayed in Fig. 2. The optimal measurement locations inside the tokamak were determined by a histogram of common separatrix midplane radii during a DIII-D run campaign, which determined that the most common separatrix locations are between $R = 2.26 - 2.29$ m. In order to produce radial profiles that capture the sharp transition from closed to open field lines, three of the sixteen channels were placed in the typical open field-line region to capture all but the most extreme case where the plasma is close to the outer limiter. Vertically viewing impurity sightlines have also been upgraded, described elsewhere[9].

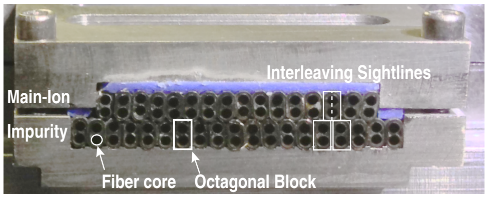

FIG. 1. Fiber clamping structure for interleaving dedicated main-ion (top) and impurity CER (bottom) sightlines.

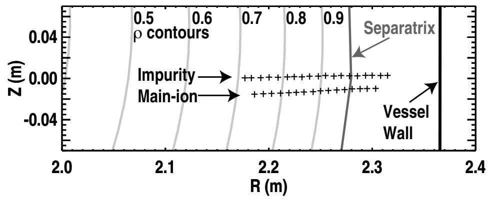

FIG. 2. Location of main-ion and impurity CER sightlines in machine and flux coordinates. Flux surface label ρ is square-root of normalized toroidal magnetic flux.

The sixteen fiber pairs are routed to two spectrometer-CCD camera systems in a manner similar to the work in Ref.[6], but with each system recording eight sightlines rather than four. Each spectrometer is a scanning Czerny-Turner type $2/3-m$ McPherson model #207 with custom asymmetric coma correction and 1200 g/mm ruled gratings. Spectral imaging is performed with SRI Avanti-768 CCD cameras with a 768 × 256 grid of 18 μm square pixels, which achieves 0.18 $\AA$/pixel reciprocal dispersion and a full spectral width of 138 $\AA$. Typical spectral acquisition is performed with 2.5 ms integration time, and integration times as low as 200 μs are possible for highest speed.

Spectroscopic analysis incorporates all active photoemission contributions to the spectrum using beam modulation background timeslice subtraction and analyzed using the fitting package described in Ref.[10], which has been described in detail previously[6,11], with two notable differences. First, inclusion of the fast-ion distribution function in the spectroscopic analysis for typical L-mode and H-mode operation is neglected. For plasmas with high density and low temperature, the contribution of the fast-ion D_α emission to the spectrum is typically negligible. Second, in the plasma core the $n = 3$ level populations are observed to be close to statistical distribution and spectral analysis is simplified by constraining the level population of each energy component to be statistical. However in the low density plasma edge the level populations deviate from a statistical distribution[12]. For the edge analysis, we fit the level populations of the full energy component, and constrain the half and third energy components to have the full energy level populations. Deviations from these assumptions are not spectroscopically resolvable and have negligible impact on the Gaussian properties of the thermal emission. The spectral data and resulting spectroscopic fit are displayed in Fig. 3 from an ELMy H-mode discharged described in the next section. It is seen that background subtraction can effectively isolate the active photoemission and leave a small residual cold emission feature, which is fit and neglected. Near the separatrix the background neutral deuterium can emit by beam-neutral impact excitation and the cold emission cannot be completely subtracted.

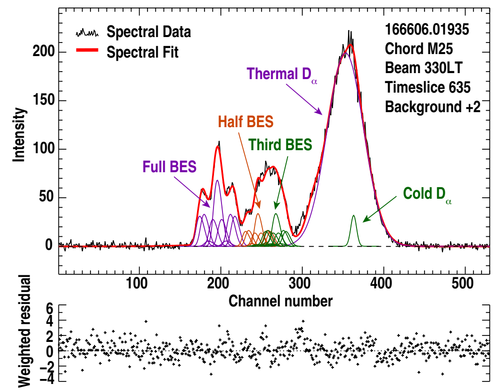

FIG. 3. Active charge-exchange spectrum and complete spectral fit.

III. PLASMA PROFILES

A type-I ELMy H-mode plasma with a configuration used extensively for pedestal and divertor physics has been executed with neutral beam timing optimized for edge charge-exchange measurements to demonstrate the performance of the edge main-ion CER system. The discharge conditions are plasma current of 1.3 MA, toroidal field of -2.0 T, neutral beam power of 3.2 MW, neutral beam torque of 3.0 Nm and normalized pressure $\beta_N = 1.9$.

Plasma profiles mapped to flux surface label ρ are displayed in Fig. 4. The electron density and temperature are obtained by Thomson scattering[13] and aligned to the separatrix by setting the electron temperature at this location to 80 eV, displayed in Fig. 4(a,b). For detailed stability and transport analysis in the H-mode pedestal, alignment of the kinetic profiles is critical because in the presence of a steep gradient, millimeter-scale systematic offsets between electron and ion density profiles produce large variations in the derived plasma Z_{eff}, collisionality and bootstrap current. Mapping of the ion profiles derived from CER relies on magnetic probes at 322°, near the measurement locations at 323° to provide an accurate determination of the magnetic separatrix with EFIT[14]. Profiles of the ion temperature from the main-ions and dominant impurity (carbon C^{+6}) are presented in Fig. 4(c). Although the temperatures are equal in the plasma core, some deviation between the species temperatures is evident near the separatrix where the density is very low. In the SOL, the carbon temperature becomes quite high and appears to identify the separatrix.

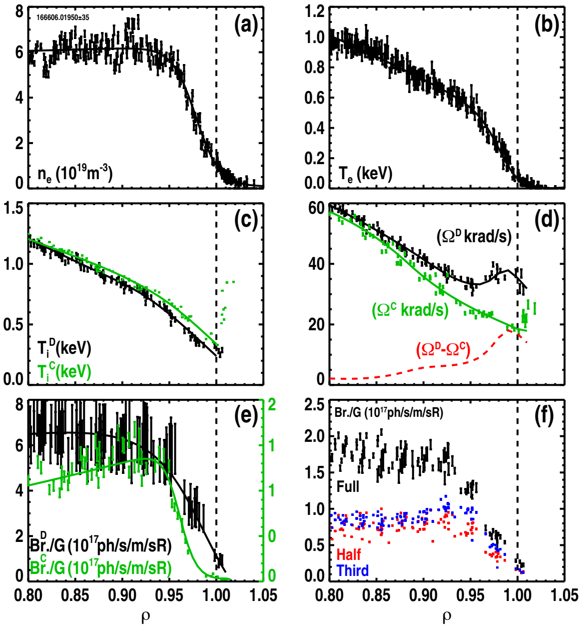

FIG. 4. H-mode pedestal profiles from Thomson scattering, impurity and main-ion CER. Detailed descriptions provided in text.

The few deuterium temperature points in the SOL indicate that the main-ion temperature should be a monotonically decreasing function of radius. Rotation of the impurities and main-ions display a much more dramatic difference. Approaching the separatrix the fluid rotation of the main-ions is significantly above that of the impurities. Displayed in Fig. 4(d) are the main-ion and impurity angular rotation speeds $\Omega \equiv V/R$, as well as the differential rotation, $\Omega^D - \Omega^C$, derived from spline fits. At the separatrix, the main-ion rotation is approximately twice that of the impurity. Capturing this difference in main-ion and impurity rotation is critical for validating theory-based models of plasma rotation that postulate the near-separatrix flow as a source of intrinsic angular momentum. Profiles of ion densities are derived from the absolute photon brightness collected by the instrument, and displaying the photon yield can reveal differences in the underlying ion density profiles. In Fig. 4(e) the wavelength-integrated spectral radiance (brightness) is displayed divided by the geometric integral of the sightline through the three-dimensional neutral beam shape. This profile is proportional to the ion density multiplied by the beam neutral density and represents the underlying ion density profile. We find that there is an apparent inward shift of the impurity emission deeper into the plasma core, which is expected by the strong neoclassical impurity convection in this region. However, the loss of the +6 carbon charge state due to low electron temperature cannot be ruled out. Deduction of the absolute ion density profiles, charge-state distributions and alignment satisfying quasi-neutrality is the subject of companion research[15]. An additional measurement provided by main-ion CER is the emission of beam neutrals resolved spectrally into their three energy components. This beam emission is used for measuring the mix of ion neutrals injected by the DIII-D heating beams[16]. Fig. 4(f) displays the emission of the full, half and third energy components caused by impact excitation of the high energy neutrals as they encounter the plasma along the ballistic injection trajectory. A noticeable shift can be seen of the peak beam emission ($\rho \approx 0.92 - 0.93$) and peak electron density ($\rho \approx 0.95$), caused by the excited state lifetime of the $n = 3$ beam neutral, which can travel 5.6 mm between excitation and emission. Taken together with Thomson scattering and impurity CER, these improvements to the DIII-D main-ion CER system provide comprehensive and detailed measurements of the fuel ion properties for integrated transport and stability analysis of the H-mode pedestal.

ACKNOWLEDGMENTS

This work supported in part by the the U.S. Department of Energy under DE-AC02-09CH11466. The author gratefully acknowledges useful discussions with R. Nazikian, W.M. Solomon, W.W. Heidbrink, M.A. Van Zeeland and E. Viezzer

[1]Y. Kim, P. H. Diamond, and R. J. Groebner, Physics of Fluids B: Plasma Physics **3**, 2050 (1991).
[2]D. J. Battaglia, K. H. Burrell, C. S. Chang, S. Ku, J. S. deGrassie, and B. A. Grierson, Physics of Plasmas (1994-present) **21**, 072508 (2014).
[3]J. S. deGrassie, S. Müller, and J. Boedo, Nuclear Fusion **52**, 013010 (2012).
[4]S. Müller, J. Boedo, K. H. Burrell, J. S. deGrassie, R. Moyer, D. Rudakov, and W. Solomon, Physical Review Letters **106**, 115001 (2011).
[5]J. Luxon, Nuclear Fusion **42**, 614 (2002).
[6]B. A. Grierson, K. H. Burrell, C. Chrystal, R. J. Groebner, D. H. Kaplan, W. W. Heidbrink, J. M. Munoz Burgos, N. A. Pablant, W. M. Solomon, and M. A. Van Zeeland, Review of Scientific Instruments **83**, 10D529 (2012).
[7]J. Boedo, E. Belli, E. Hollmann, W. M. Solomon, D. L. Rudakov, and K. H. Burrell, Physics of Plasmas **18** (2011).
[8]P. Gohil, K. H. Burrell, R. J. Groebner, and R. Seraydarian, Review of Scientific Instruments **61**, 2949 (1990).
[9]C. Chrystal, Rev. Sci. Instrum (2016), submitted for publication.
[10]N. A. Pablant, K. H. Burrell, R. J. Groebner, D. Kaplan, and C. T. Holcomb, Review of Scientific Instruments **79**, 10F517 (2008).
[11]B. A. Grierson, K. H. Burrell, W. W. Heidbrink, M. J. Lanctot, and N. A. Pablant, Physics of Plasmas **19**, 056107 (2012).
[12]O. Marchuk, Y. Ralchenko, R. Janev, W. Biel, E. Delabie, and A. Urnov, Journal of Physics B: Atomic, Molecular and Optical Physics **43**, 011002 (2010).
[13]D. Eldon, B. D. Bray, T. M. Deterly, C. Liu, M. Watkins, R. J. Groebner, A. W. Leonard, T. H. Osborne, P. B. Snyder, R. L. Boivin, and G. R. Tynan, Review of Scientific Instruments **83**, 10E343 (2012).
[14]L. Lao, H. S. John, R. Stambaugh, A. Kellman, and W. Pfieffer, Nucl. Fusion , 1611 (1985).
[15]S. R. Haskey, Rev. Sci. Instrum (2016), submitted for publication.
[16]B. A. Grierson, K. H. Burrell, B. Crowley, L. Grisham, and J. T. Scoville, Review of Scientific Instruments **85**, 103502 (2014).

Princeton Plasma Physics Laboratory
Office of Reports and Publications

Managed by
Princeton University

under contract with the
U.S. Department of Energy
(DE-AC02-09CH11466)

P.O. Box 451, Princeton, NJ 08543
Phone: 609-243-2245
Fax: 609-243-2751

E-mail: publications@pppl.gov

Website: http://www.pppl.gov